Optical and structural properties of MeV erbium-implanted $LiNbO_3$

M. Fleuster and Ch. Buchal
Institut für Schicht- und Ionentechnik (ISI), Forschungszentrum Jülich, D-5170 Jülich, Germany

E. Snoeks and A. Polman
FOM-Institute for Atomic and Molecular Physics, Kruislaan 407, 1098 SJ Amsterdam, The Netherlands

(Received 5 August 1993; accepted for publication 28 September 1993)

$LiNbO_3$ single crystals have been implanted with 2.0 or 3.5 MeV Er ions with fluences between 2.0×10^{14} and 7.5×10^{15} cm^{-2} and annealed at temperatures between 500 and 1060 °C in a wet oxygen atmosphere. Photoluminescence spectroscopy, Rutherford backscattering spectroscopy, and secondary-ion-mass spectrometry have been used to study the influence of the annealing treatment on the optical activity of the Er ions, the crystal structure of the implanted $LiNbO_3$ layer, and the depth distribution of the Er ions, respectively. The as-implanted, amorphized $LiNbO_3$ already emits the characteristic photoluminescence (PL) of Er^{3+} around 1.53 μm. Annealing for 1 min at 500 °C causes recrystallization of the amorphized layer by columnar solid-phase epitaxial regrowth from the substrate. The PL intensity increases by more than one order of magnitude on annealing at 500 °C and the PL lifetime rises from 1.65 to 2.85 ms. In contrast, much longer annealing times and a much higher temperature are necessary to remove the columns and restore the perfect lattice but do not further improve the optical properties. Up to an Er concentration of 0.12 at. % no concentration quenching effects are noticed. MeV implantation-doped samples show the same optical spectra as those doped during growth from the melt.

I. INTRODUCTION

Er-doped materials have recently achieved great importance for application in optical communication devices because the Er ion shows an optical (intra-$4f$) transition around 1.5 μm which coincides with the low-loss window of standard optical telecommunication fibers. The excellent performance of Er-doped fiber amplifiers stimulates efforts to also optically activate materials used in planar integrated optics by incorporating Er. In particular, the doping of $LiNbO_3$ is an interesting task because it enables the combination of the optically active Er ions with the excellent nonlinear, electro-optical, and acousto-optical properties of $LiNbO_3$. Optical devices such as waveguide lasers (mode locked, Q switched, self-frequency doubled, tunable) and waveguide amplifiers can in principle be realized and the monolithic integration of passive and active devices on one chip may become possible. Indeed waveguide lasers and amplifiers in Er-doped $LiNbO_3$ have already been fabricated.[1,2] Recently, the first mode-locked waveguide laser based on Er-doped $LiNbO_3$ was presented.[3]

When incorporated in the trivalent state (Er^{3+}: $4f^{11}$ configuration) into a solid host, the Er ions can emit light around 1.5 μm,[4,5] corresponding to transitions between the first excited manifold $^4I_{13/2}$ and the $^4I_{15/2}$ ground-state manifold (Fig. 1). Practical pump bands are the transitions from the ground state into the $^4I_{9/2}$, $^4I_{11/2}$, and $^4I_{13/2}$ levels[6] since lasers at 800, 980, and 1480 nm are commercially available. After excitation the ion rapidly decays to the first excited manifold by nonradiative decay. This optical system is a three-level system because the lower level of the 1.5 μm transition is identical to the ground state, and as a result high pump powers are necessary to achieve inversion. Additionally, the 1.5 μm signal will be reduced by ground-state absorption if in an Er-doped part of the waveguide the pump power is not sufficient to provide inversion. Consequently the threshold pump power of potential waveguide lasers and amplifiers—using the Er ions as a gain medium—depends critically on the shape and the position of the Er depth profile (relative to that of the pump and signal mode). In the case of a monomode waveguide the threshold pump power can be minimized by placing the Er ions in the center of the waveguide where the pump intensity has its maximum.

Up to now the $LiNbO_3$ substrates used for the fabrication of waveguide lasers and amplifiers have been doped with Er by in-diffusion from an evaporated Er film. The performance of these devices is still far from the theoretical optimum because the overlap between Er profile and optical modes is rather poor: the in-diffusion leads to an Er depth profile which can be described by an erfc(x/D) function,[7] causing the maximum concentration to be at the surface. There, on the other hand, the pump intensity is close to zero. In this article we show that MeV implantation is an attractive alternative approach to incorporate Er into $LiNbO_3$. It allows the tuning of the Er profile on a micron depth scale, the typical dimension of optical waveguides. Indeed, in an earlier publication[8] we have shown that the MeV-implanted Er profile, better tailored to the optical modes than the in-diffused one, promises a significant reduction (up to a factor of 5) in the threshold pump power of waveguide lasers and amplifiers. Furthermore, implantation is independent of the thermodynamical restrictions which limit the maximum concentration achievable by indiffusion. Higher concentrations would allow for shorter or more efficient devices. Optical activation of Er incorporated by implantation has been shown to be

 0021-8979/94/75(1)/173/8/$6.00

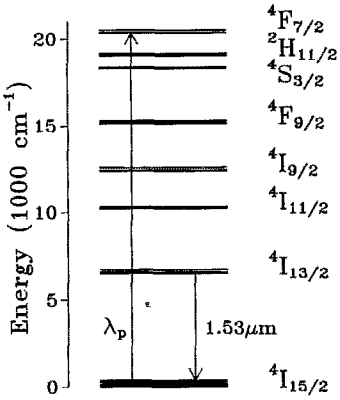

FIG. 1. Intra-4f energy-level diagram of the Er^{3+} ion in a $LiNbO_3$ host (see Ref. 5). The levels are split into manifolds due to the Stark effect. λ_P indicates the pump transition.

possible in different optical waveguiding materials such as SiO_2,[9] Si_3N_4,[9] Al_2O_3,[10] and silicate glasses.[11]

In this work we study the annealing characteristics of 3.5 MeV Er-implanted $LiNbO_3$ single crystals. Photoluminescence spectroscopy together with Rutherford backscattering spectrometry is used to investigate the dependence of the optical properties of the Er ions on the defect structure of the $LiNbO_3$ host and on Er concentration. As a result of the implantation the $LiNbO_3$ single crystals are amorphized to a depth of 1.25 μm. Annealing for 1 min at 500 °C causes the recrystallization of the amorphized layer by columnar solid-phase-epitaxial (SPE) regrowth from the substrate and to fully optically activate the Er ions. In contrast, a much longer annealing time and higher annealing temperature are necessary to restore the single-crystalline quality. No concentration quenching effects are noticed up to an Er concentration of 0.12 at. %.

II. EXPERIMENT

Commercially available x-cut $LiNbO_3$ single crystals (Crystal Technology) with the dimensions $1\times5\times10$ mm^3 were implanted at room temperature with 2 or 3.5 MeV Er ions, using a 1 MV van de Graaff or a 1.7 MV tandetron accelerator. During implantation the crystals were tilted by 7° to avoid channeling and heat sunk to a copper block. The beam was scanned through an aperture of typically 1×1 cm^2 size, resulting in a beam current density on the target of typically 0.25 μA/cm^2. The implantation fluences ranged from 2.0×10^{14} to 7.5×10^{15} ions/cm^2. Thermal annealing was performed either in a quartz tube furnace (for anneals longer than 5 min) in a wet oxygen atmosphere to suppress Li outdiffusion[12] or in a rapid thermal annealer (RTA) under flowing O_2. The given annealing times for the RTA samples are the real holding times; the sample defined as "0 s" was just heated up to the final temperature and immediately cooled down again.

The annealing behavior of the damaged $LiNbO_3$ lattice after implantation was studied using Rutherford backscattering spectrometry (RBS) and channeling parallel to the x-axis with 3 MeV He^{++} ions at a scattering angle of 170° resulting in a depth resolution of 200 Å. In addition, as-implanted and annealed samples were analyzed by transmission electron microscopy (TEM) using a 100 kV electron microscope. Plan-view specimens were prepared by mechanical polishing and ion-milling thinning. The Er concentration profiles were determined by secondary-ion-mass spectrometry (SIMS), using O^+ to sputter an area of 150×150 μm^2. Only those sputtered ions originating from a central circular area of 8 μm diameter were analyzed. To avoid charging a thin gold film was evaporated on top of the insulating $LiNbO_3$ samples; charging of the sputter crater during the measurement was compensated for by an electron beam directed to the sputtered region. In order to obtain quantitative results the Er signal was normalized to the Nb yield; an Er:$LiNbO_3$ single crystal, doped homogeneously (0.03 at. % Er) during growth from the melt served as a standard. This sample was also used as a reference for the optical measurements.

Photoluminescence (PL) spectrometry was performed at room temperature and 77 K, using the 496.5 and 488 nm line of an Ar-ion laser as excitation source, respectively. Both lines are absorbed in the $^4F_{7/2}$ manifold of the Er^{3+} ion (see Fig. 1). Using these lines resulted in the maximum PL intensity at the corresponding temperature. Powers between 100 and 250 mW were used; the signal was analyzed with a 48 cm monochromator and detected by a liquid-nitrogen-cooled Ge detector, yielding a spectral resolution ranging from 2 to 32 Å. The pump beam was mechanically chopped at 10 Hz and the signal was collected using a lock-in amplifier. Time-resolved luminescence decay measurements were carried out using a 1.5 ms, 500 mW pulse with a cut-off time shorter than 150 μs, also obtained by mechanical chopping.

III. RESULTS

A. Structural characterization

Figure 2 shows the ion-channeling spectra of $LiNbO_3$ single crystals implanted with a fluence of 5×10^{15} Er/cm^2 at 3.5 MeV and annealed at 500 °C for different times using the RTA. Also shown is the random spectrum of the as-implanted sample. The channeling spectrum of the as-implanted sample (not shown) is indistinguishable from the 0 s sample. The spectra are dominated by the Nb signal, the Er concentration being too low to give a significant contribution. The step at channel 350 is caused by the O signal. For the as-implanted sample the channeling yield in the 1.25-μm-thick surface region is identical to the random yield, indicating it is highly disordered. TEM (shown further on) shows that the as-implanted surface layer is fully amorphous. With the onset of annealing the interface between the amorphous surface region and the deeper crystalline region starts to move to the surface with a speed of (320 ± 50) Å/s. After ~40 s at 500 °C the surface has been reached, but a large amount of residual damage is still present. Longer annealing at this temperature does not further change the channeling spectrum.

To remove the residual damage, annealing treatments at much higher temperatures are necessary. The RBS

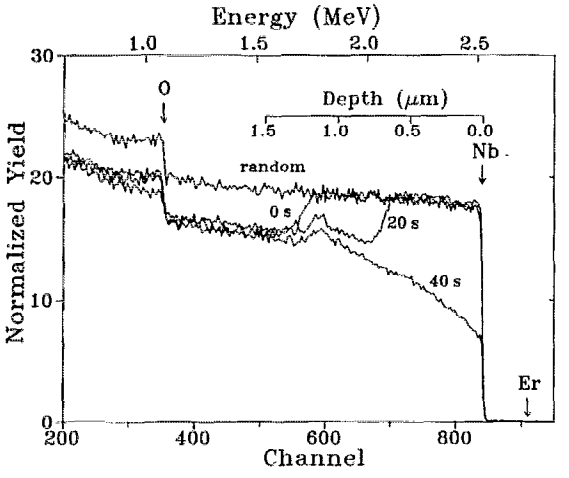

FIG. 2. RBS channeling spectra of Er-implanted (3.5 MeV, 5×10^{15} Er/cm^2) $LiNbO_3$ single crystals, annealed for different times at 500 °C in flowing oxygen using a RTA. The channeling spectrum of the as-implanted sample (not shown) is indistinguishable from the spectrum of the 0 s sample. Also shown is the random spectrum of the as-implanted sample. The arrows indicate surface channels of the different constituents.

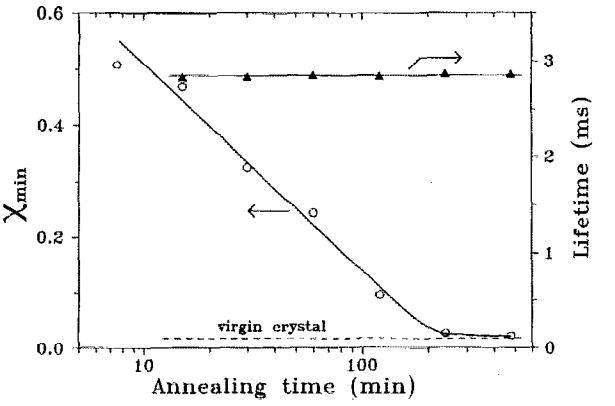

FIG. 4. Minimum yield χ_{min} value as function of annealing time at 1060 °C for the same set of samples as in Fig. 3 (○, left-hand-side axis). These values have been derived from the channeling spectra of Fig. 3. Note the logarithmic scale of the time axis. The dashed line indicates the χ_{min} value of a virgin crystal. Also given is the photoluminescence lifetime, measured at 1533 nm (▲, right-hand-side axis). The solid lines serve as guides to the eye.

channeling spectra after annealing in the tube furnace at 1060 °C for times up to 4 h are shown in Fig. 3. The channeling yield continuously decreases in the implanted region with increasing annealing time. For each spectrum the minimum yield χ_{min} was calculated, defined as the average yield between the channels 800 and 830 normalized to the random yield. Figure 4 summarizes these values as function of annealing time at 1060 °C (left-hand-side axis, open circles). As can be seen χ_{min} decreases linearly on a logarithmic time scale. After 4 h annealing at 1060 °C χ_{min} has improved to 2.8%, quite close to the value of a virgin crystal ($1.8\pm0.3\%$) which is indicated by the dashed line. A further increase of annealing time to 8 h results in a channeling spectrum that is indistinguishable from the virgin spectrum, manifesting the excellent crystal quality of the MeV-implantation Er-doped $LiNbO_3$. Anneals at 950 °C were also performed; at this temperature the χ_{min} value saturates at about 30% for long annealing.

The electron-diffraction pattern of the as-implanted sample is shown in Fig. 5(a). A ring pattern can be seen, showing that the implanted region is amorphous. Figure 5(b) shows the plan-view bright-field image of the sample annealed at 1060 °C for 15 min. It reveals grains with a typical size of 0.5–1.5 μm. The corresponding diffraction pattern of the whole area, shown in Fig. 5(c), demon-

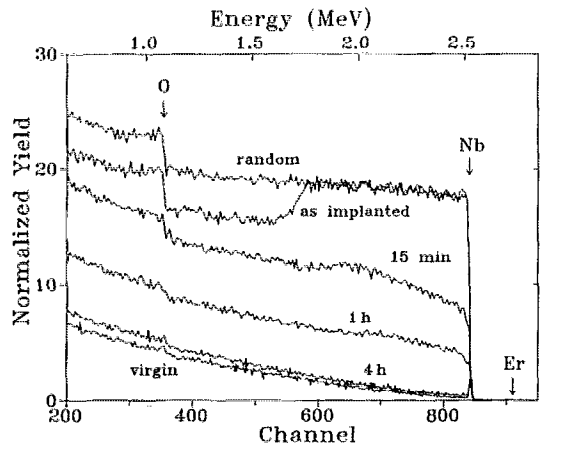

FIG. 3. RBS channeling spectra of Er-implanted (3.5 MeV, 5×10^{15} Er/cm^2) $LiNbO_3$ single crystals, annealed for different times at 1060 °C in a wet oxygen atmosphere. Also shown is the random spectrum of the as-implanted sample.

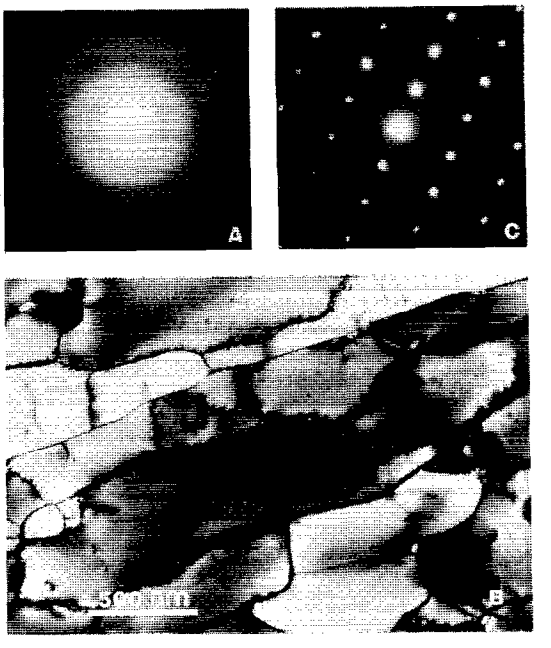

FIG. 5. (a) Electron-diffraction pattern of a $LiNbO_3$ single crystal implanted with 5×10^{15} Er/cm^2 at 3.5 MeV, (b) plan-view bright-field image of a sample implanted identically after annealing for 15 min at 1060 °C, and (c) the corresponding diffraction pattern of the whole area.

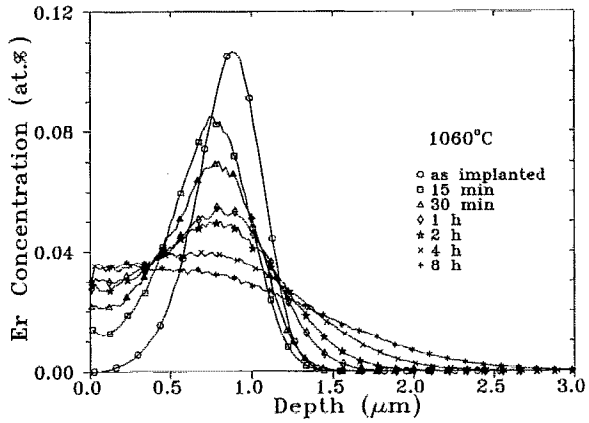

FIG. 6. SIMS depth profiles of Er-implanted (3.5 MeV, 5×10^{15} Er/cm^2) $LiNbO_3$ single crystals, annealed for different times at 1060 °C in a wet oxygen atmosphere. From these profiles a diffusion constant of $(8\pm1)\times10^{-14}$ cm^2/s has been derived.

strates that all grains are crystalline and all have the same orientation.

To study the possible redistribution of Er during the high-temperature annealing treatment, SIMS measurements were performed on a second set of samples similar to those of Fig. 3. The results are shown in Fig. 6. The as-implanted profile is nearly Gaussian shaped, and peaks at a depth of 0.89 μm from the surface with a full width at half maximum (FWHM) of 0.46 μm. The peak concentration is 0.11 at. %. After 15 min at 1060 °C the peak of the Er profile has shifted slightly closer to the surface and widened significantly. With increasing annealing time the Er ions diffuse toward the surface and into the bulk. As a result of reflection at the surface the Er profile becomes flat near the surface for long annealing treatments. After 4 h the maximum concentration has been reduced to 0.04 at. %. The Er profiles can be described quite accurately using a standard Fick's diffusion model, with a concentration-independent diffusivity of $(8\pm1)\times10^{-14}$ cm^2/s. Not explained by this model are the shift of the concentration peak during the first minutes of annealing and the surface concentration which is slightly higher than expected.

B. Optical characterization

Room-temperature PL spectra of samples implanted with 5×10^{15} Er/cm^2 at 3.5 MeV and annealed at 500 °C for different times using RTA are given in Fig. 7. These samples are identical to the samples in Fig. 2. Already the as-implanted sample shows a measurable PL signal at room temperature. The spectrum consists of a few very broad lines and peaks at 1.533 μm. For this sample a time-dependent behavior during PL excitation was found: During illumination (2 h with 250 mW at 496.5 nm) the PL intensity slowly increased by about a factor of 5. Such a time-dependent effect was not observed for annealed samples.

During annealing at 500 °C the shape of the spectrum changes dramatically: While the 0 s sample still emits the

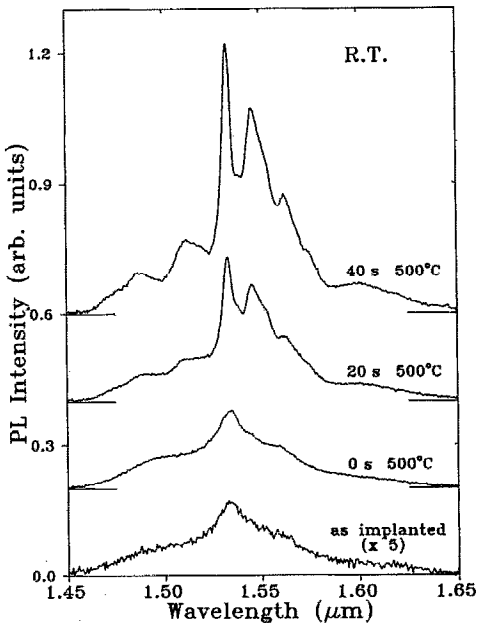

FIG. 7. Room-temperature photoluminescence spectra of Er-implanted (3.5 MeV, 5×10^{15} Er/cm^2) $LiNbO_3$ single crystals annealed for different times at 500 °C in flowing oxygen using the RTA. A pump power of 100 mW, a pump wavelength of 496.5 nm, and a spectral resolution of 3.2 nm were used. The spectra have been shifted vertically for clarity. The absolute intensities can be compared directly, only the spectrum of the as-implanted sample has been scaled with a factor of 5.

same spectrum as the as-implanted one, after annealing for 20 s the shape gets much more structured. After 40 s the spectrum consists of different well-defined lines. All observed photoluminescence lines correspond to transitions between the $^4I_{13/2}$ and $^4I_{15/2}$ manifolds of the Er^{3+} ion—both split by the crystal field (Stark splitting) of the $LiNbO_3$ host—and can be assigned on the basis of the term scheme given by Gabrielyan and co-workers.[5] The most intense line at 1.533 μm originates from the transition between the lowest Stark levels of both multiplets, respectively. Longer annealing at this temperature does not change the shape of the spectra; only the linewidth of the peak at 1.533 μm is further reduced. It is interesting to compare these results with the annealing behavior of the $LiNbO_3$ host (see Fig. 2): after 40 s the interface has reached the surface and the shape of the PL spectrum has achieved its final state. For all spectra of Fig. 7 the PL intensity was integrated between 1.45 and 1.65 μm and plotted in Fig. 8. On heating up to 500 °C (0 s sample) the PL intensity increases by a factor of 5 compared to that of the as-implanted sample. During the next 40 s the intensity further increases twofold. A very slight further increase is observed for longer annealing times (500 °C, 5 min).

Figure 9 shows PL spectra after annealing at 1060 °C (15 min and 8 h). For comparison the spectrum after annealing at 500 °C for 5 min is included. As can be seen, annealing at the much higher temperature leads to a very similar spectrum. Some of the peaks become somewhat more pronounced and the integrated intensity increases by an additional 10% compared to the sample annealed at

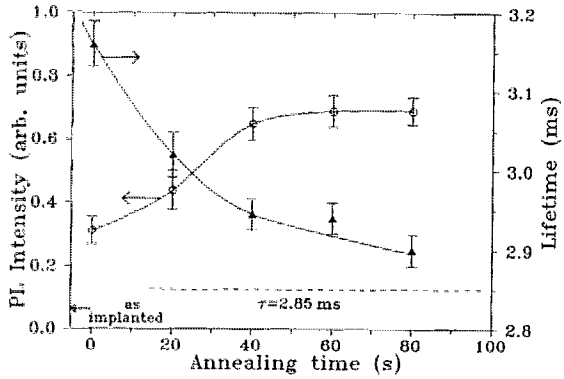

FIG. 8. Integrated photoluminescence intensity (between 1.45 and 1.65 μm, ○, left-hand-side axis) and lifetime at 1.533 μm (▲, right-hand-side axis) as a function of annealing time at 500 °C. All samples have been implanted with 5×10^{15} Er/cm^2 at 3.5 MeV. The PL intensity for the as-implanted sample is indicated by an arrow. The dashed line indicates the lifetime of the samples annealed at 1060 °C (see Fig. 4); the solid lines serve as guides to the eye.

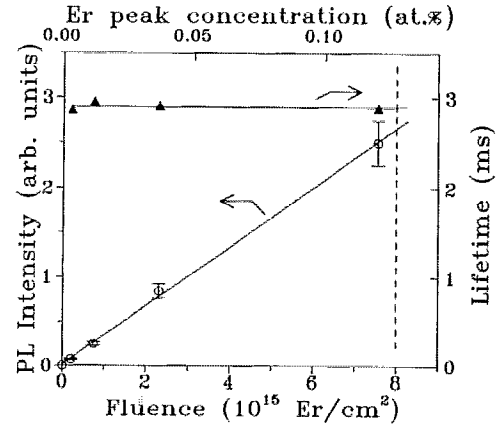

FIG. 10. Photoluminescence intensity (○, left-hand-side axis) and lifetime (▲, right-hand-side axis) at 1533 nm as a function of Er fluence. All samples have been implanted with 2 MeV and annealed for 4 h at 1060 °C in a wet oxygen atmosphere. The Er peak concentration is indicated on the top axis. The solid lines are linear least-mean-square fits, the dashed vertical line marks the maximum Er concentration which can be achieved by diffusion (see Ref. 7).

500 °C for 5 min. Already the sample annealed for 15 min at 1060 °C shows the finally shaped spectrum and the full integrated intensity. No changes in the intensity and the shape of the spectra—i.e., the relative height, position, and linewidth of the peaks—are observed during further annealing.

Fluorescence decay measurements at 1533 nm were performed for all samples. In all cases a single-exponential decay of the photoluminescence signal was found. The measured $1/e$ decay time of the high-temperature-annealed samples as function of the annealing time is given in Fig. 4 for comparison with the χ_{min} data. All samples exhibit the same lifetime of (2.85 ± 0.03) ms while the χ_{min} value gradually decreases. The lifetimes of the samples annealed at 500 °C are depicted in Fig. 8. Not shown is the lifetime of the as-implanted sample which is (1.65 ± 0.15) ms. When the sample has reached the final temperature of 500 °C (0 s) the lifetime has nearly doubled to 3.16 ms. During further annealing the lifetime gradually decreases and approaches the value which was found for the samples annealed at 1060 °C (indicated by the dashed line) and reaches this value after 5 min.

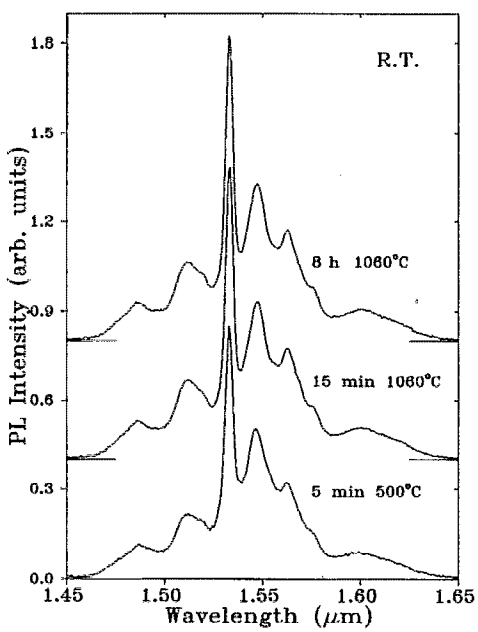

FIG. 9. Room-temperature photoluminescence spectra of Er-implanted (3.5 MeV, 5×10^{15} Er/cm^2) $LiNbO_3$ single crystals annealed at different annealing conditions. A pump power of 100 mW, a pump wavelength of 496.5 nm, and a spectral resolution of 3.2 nm were used. The spectra have been shifted vertically for clarity. The absolute intensities can be compared directly.

The concentration dependence of the optical properties of Er-doped $LiNbO_3$ was studied using samples implanted with Er fluences between 2.0×10^{14} and 7.5×10^{15} ions/cm^2 at 2 MeV and then annealed for 4 h at 1060 °C in the tube furnace. The shape of the PL spectra found for these samples is identical to the shapes shown in Fig. 9 and does not depend on Er concentration. In Fig. 10 PL intensity and lifetime, both measured at 1533 nm, are plotted against the Er fluence. The Er peak concentration derived from SIMS data is given at the top axis. The PL intensity increases linearly with Er concentration, while the lifetime is constant over the whole concentration range. The dashed line in Fig. 10 indicates the maximum Er concentration that can be incorporated into $LiNbO_3$ by Er in-diffusion at 1060 °C.[7]

Finally, we compare the optical quality of MeV-implanted $LiNbO_3$ with that of $LiNbO_3$ doped with Er during growth from the melt. PL-measurements at 77 K using a spectral resolution of 2 Å were performed. The spectra of a 3.5-MeV-implanted (annealed for 15 min at 1060 °C) sample and a melt-doped Er:$LiNbO_3$ single crystal (0.03 at. % Er) are shown in Fig. 11. Due to the fact that the total areal density of Er ions in the melt-doped sample is about three orders of magnitude higher than for the implanted one, the signal-to-noise ratio is much better

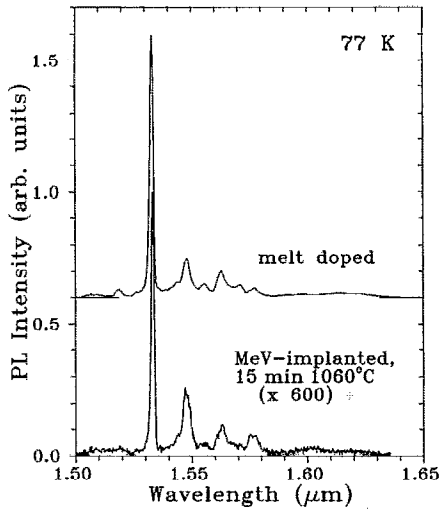

FIG. 11. 77 K photoluminescence spectra of an Er-implanted (3.5 MeV, annealed for 15 min at 1060 °C) and a melt-doped $LiNbO_3$ single crystal. A pump power of 250 mW, a pump wavelength of 488.0 nm, and a spectral resolution of 0.2 nm were used.

for the former one. Nevertheless, it can easily be seen that the position of the different luminescence lines, their relative heights, and their widths are identical for both spectra. In addition, the lifetime of (2.85 ± 0.03) ms measured for the MeV-implantation-doped samples is only marginally lower than that of the melt-doped crystal (2.95 ms).

IV. DISCUSSION

The experimental data indicate that the behavior of MeV Er-implanted $LiNbO_3$ during annealing is determined by two different annealing characteristics. Annealing for a short time at a low temperature (500 °C) is sufficient to fully optically activate the incorporated Er ions as shown in Fig. 7. In contrast, 8 h at 1060 °C is necessary to anneal out all implantation-induced damage and restore the single-crystal quality (Fig. 3).

A. Structural properties

The channeling data of Fig. 2 show that at 500 °C the amorphized surface layer recrystallizes by the movement of the amorphous-crystalline interface. Such SPE regrowth of ion-implanted $LiNbO_3$ was observed earlier,[13] and indeed the growth rates observed in our work agree with values for undoped material extrapolated from earlier work. This indicates that the presence of Er does not influence the SPE regrowth rate, at least up to the concentrations used here. With the regrowth completed, ion channeling still detects a high level of residual damage. As shown by the plan-view TEM micrographs, SPE takes place via columnar growth, with a large density of grain boundaries. These grain boundaries cause dechanneling in RBS which results in the high $\chi_{\min}$ value after 500 °C annealing. They are very stable and long annealing at 1060 °C is necessary to remove them.

An important conclusion from this work is that the defects remaining after 500 °C annealing (i.e., with the regrowth completed) do not influence the Er luminescence. In addition, they do not change the diffusivity of Er in comparison to that for single-crystalline material: The diffusion constant of $(8\pm1)\times10^{-14}$ cm^2/s derived from the SIMS spectra of Fig. 6, agrees very well with the value of $(6.6\pm0.9)\times10^{-14}$ cm^2/s found for Er diffusion at 1060 °C parallel to the x axis in a $LiNbO_3$ single crystal.[7]

B. Optical properties

The shape of the PL spectrum of Er-implanted $LiNbO_3$ (Fig. 7) changes from a very broad spectrum to separate sharp peaks during annealing at 500 °C. Due to the Stark effect the shape of the PL spectrum is a sensitive probe for the local surrounding of the Er ion. Therefore, this change in the shape of the spectrum is consistent with the observation of SPE. In the as-implanted sample and still after 0 s annealing, some Er is in the trivalent, optically active state, but surrounded by amorphous $LiNbO_3$ resulting in a strongly inhomogeneously broadened spectrum. During further annealing (up to 40 s), regrowth of the $LiNbO_3$ takes place and the peaks in the spectra become sharper, showing that the local surrounding of all Er ion become similar.

From rate equation arguments, it follows that the photoluminescence intensity is proportional to the lifetime τ of the $I_{13/2}$ manifold and to the number of optically active (trivalent) Er ions per area N_{Er}

$$I \propto \frac{\tau}{\tau_r} N_{\mathrm{Er}}. \tag{1}$$

The measured lifetime τ is determined by the radiative (τ_r^{-1}) and nonradiative (τ_{nr}^{-1}) decay rates, respectively,

$$\frac{1}{\tau}=\frac{1}{\tau_r}+\frac{1}{\tau_{\mathrm{nr}}}. \tag{2}$$

These equations are used to explain the behavior of PL intensity and lifetime during annealing at 500 °C. The as-implanted sample shows a low PL signal and a lifetime of 1.64 ms. By heating the sample up to 500 °C (0 s) the lifetime doubles and the PL intensity increases fivefold. The doubling of the lifetime is a result of the annihilation of some of the implantation-induced defects that couple to the excited Er ions and quench the PL intensity and lifetime via nonradiative decay. According to Eq. (1) this can only account for a doubling in PL intensity, but the increase is fivefold. Therefore, the number of active Er ions must simultaneously increase. During the SPE regrowth the number of active Er ions further increases, as indicated in Fig. 8 by the further increase in PL intensity for longer annealing at 500 °C. The gradual decrease in the lifetime during the recrystallization (see Fig. 8) may be caused by several effects: first, by changing the local surrounding the radiative decay rate (τ_r^{-1}) can be influenced. Second, it is known that the refractive index n_0 (n_e) of amorphized $LiNbO_3$ implanted at 300 K is 6% (2%) lower than that of single-crystalline material.[14] A lower index will cause a lower optical mode density and therefore a longer radiative lifetime ($\tau_r^{-1}\sim n^2$). Third, some Li out-diffusion may have

taken place during implantation of $LiNbO_3$. A Li deficit may influence the lifetime. Indeed, for Eu-doped $LiNbO_3$ an influence of the Li/Nb ratio on the optical properties of the Eu ions has been observed.[15]

The annealing treatment at 1060 °C, which is necessary to remove the residual damage, has no significant effect on the PL properties. The measurements at 77 K (Fig. 11) show that for the sample annealed for 15 min at 1060 °C all peaks can be clearly separated. This implies that the linewidth at room temperature is largely determined by homogeneous broadening. Based on these observations it can be concluded that with the regrowth completed the optical properties of the Er ions have reached their final state. The still existing residual damage does not couple to the excited Er ions.

The PL lifetime τ of the Er ions is independent of the fluence in the concentration range studied here (Fig. 10). In this case Eq. (1) predicts a linear increase of the PL intensity as a function of the number of optically active Er ions. Indeed, the PL intensity was found to increase linearly with Er fluence indicating that the active fraction of the Er ions is the same for all fluences. Both experimental facts prove the total absence of any concentration quenching effects—such as energy transfer between Er ions or cooperative upconversion—up to the highest peak concentration of 0.12 at. %. An additional indication of a concentration-independent luminescence lifetime follows implicitly from Figs. 4 and 6: While diffusion reduces the peak concentration from 0.085 at. % after 15 min annealing at 1060 °C to 0.035 at. % after 8 h the lifetime and the intensity remain constant as a function of annealing time. Additional work has been started to further increase the implanted Er fluence and to characterize the Er–Er interactions which are expected to limit the device performance in the high dopant concentration regime.

The similarity of the spectra (Fig. 11) for melt-doped and MeV-implanted Er:$LiNbO_3$ indicates that the Er lattice site is the same for both crystals. Work on melt-doped and indiffused $LiNbO_3$ has shown that Er is incorporated into an octahedral position close to the Li site,[16,17] surrounded by six oxygen ions. The nearly identical lifetimes (2.97 versus 2.85 ms) prove that the implantation-induced point defects—at least those that can couple to the excited Er ions—have been annealed out completely. Both facts emphasize that optical doping of $LiNbO_3$ by MeV implantation leads to the same PL properties as doping during growth from the melt or indiffusion. In an earlier publication[8] we already presented a calculation which showed that the resulting Er profile after 4 h annealing at 1060 °C [necessary to restore the perfect lattice (Fig. 3)] promises a significant improvement in the performance of waveguide lasers and amplifiers. An even more dramatic progress can be expected if the low-temperature (500 °C) annealed crystals could be used: After 1 min at 500 °C the Er profile is still very close to the Gaussian shape of the as-implanted profile. Therefore, the matching to the optical modes will be further improved as compared to the long-time (4 h) annealed samples. Studies to investigate the influence of the residual damage still present after 500 °C annealing on waveguide losses have been started.

V. CONCLUSION

This study shows that MeV ion implantation is a suitable method for the incorporation of Er ions into an optically active site in $LiNbO_3$. The PL spectra and the lifetime of the $I_{13/2}$ level are the same as for a melt-doped sample. This proves that the occupied lattice site is the same and that the implantation-induced defects which quench luminescence have been annealed out. The annealing characteristics of Er-implanted $LiNbO_3$ involve two different effects: Only 40 s annealing at 500 °C is enough to recrystallize the implanted, amorphized layer by columnar SPE regrowth from the substrate and to fully optically activate the implanted Er ions. Annealing for 4 h at 1060 °C is necessary to remove the grain boundaries between the columns and to restore the crystal quality to that of a virgin crystal. No concentration quenching effects were observed up to a maximum concentration of 0.12 at. %. This value is a typical concentration used in waveguide devices. In contrast to other techniques such as indiffusion or melt doping, MeV ion implantation allows tailoring of the Er depth profile to the special demands of an optical device. The improved overlap between Er profile and optical modes promises higher gain values and lower threshold pump powers for Er:$LiNbO_3$-based amplifiers and lasers as compared to the devices realized so far by the indiffusion of Er.

ACKNOWLEDGMENTS

We thank H. Holzbrecher and U. Breuer from ZCH of KFA Jülich for performing the SIMS measurements. We gratefully acknowledge the support from the Tandetron facility and staff at IFF of KFA Jülich. J. S. Custer is acknowledged for transmission electron microscopy and for helpful discussion. The Dutch part of this work is part of the research program of the Foundation for Fundamental Research on Matter (FOM) and was made possible by financial support from the Dutch organization for the Advancements of Pure Research (NWO), the Netherlands Technology Foundation (STW), and the IC Technology Program (IOP Electro-optics) of the ministry of Economic Affairs.

[1] R. Brinkmann, W. Sohler, and H. Suche, Electron. Lett. **27**, 415 (1991).
[2] P. Becker, R. Brinkmann, M. Dinand, W. Sohler, and H. Suche, Appl. Phys. Lett. **61**, 1257 (1992).
[3] H. Suche, I. Baumann, D. Hiller, and W. Sohler, in Proceedings of the European Conference on Integrated Optics (ECIO), Neuchâtel, April 1993, postdeadline paper 3.
[4] S. Hüfner, *Optical Spectra of Transparent Rare-Earth Compounds* (Academic, New York, 1978).
[5] V. T. Gabrielyan, A. A. Kaminskii, and L. Li, Phys. Status Solidi A **3**, K37 (1970).
[6] W. J. Miniscalco, IEEE J. Lightwave Technol. **LT-9**, 234 (1991).

[7] I. Baumann, R. Brinkmann, Ch. Buchal, M. Dinand, M. Fleuster, H. Holzbrecher, W. Sohler, and H. Suche, in Proceedings of the European Conference on Integrated Optics (ECIO), Neuchâtel, April 1993, pp. 3–14.
[8] M. Fleuster, Ch. Buchal, H. Holzbrecher, U. Breuer, M. Dinand, H. Suche, R. Brinkmann, and W. Sohler, Mater. Res. Soc. Symp. Proc. **279**, 279 (1993).
[9] A. Polman, D. C. Jacobson, D. J. Eaglesham, R. C. Kistler, and J. M. Poate, J. Appl. Phys. **70**, 3778 (1991).
[10] G. N. van den Hoven, E. Snoeks, A. Polman, J. W. M. van Uffelen, Y. S. Oei, and M. K. Smit, Appl. Phys. Lett. **62**, 3065 (1993).
[11] E. Snoeks, G. N. van den Hoven, and A. Polman, J. Appl. Phys. **73**, 8179 (1993).
[12] J. L. Jackel, J. Opt. Commun. **3**, 82 (1982).
[13] D. B. Poker and D. K. Thomas, J. Mater. Res. **4**, 412 (1989).
[14] G. L. Destefanis, J. P. Gaillard, E. L. Ligeon, S. Valette, B. W. Farmery, P. D. Townsend, and A. Perez, J. Appl. Phys. **50**, 7898 (1979).
[15] J. E. Muñoz Santiuste, B. Macalik, and J. García Solé, Phys. Rev. B **47**, 88 (1993).
[16] L. Rebouta, M. F. da Silva, J. C. Soares, J. A. Sanz-Garcia, E. Dieguez, and F. Agullo-Lopez, Nucl. Instrum. Methods B **64**, 189 (1992).
[17] T. Gog, M. Griebenow, and G. Materlik (unpublished).